

# **Thermodynamic Analysis of Integrated Oxy-combustion Supercritical CO<sub>2</sub> Power Cycle with Concentrated Solar Power**

**Foyez Ahmad, Fardin Mahatab and Sajjad Mahmud**

Department of Mechanical and Production Engineering

Islamic University of Technology (IUT)

Board Bazar, Gazipur, Dhaka, Bangladesh

foyezahmad@iut-dhaka.edu, fardinmahatab@iut-dhaka.edu, sajjadmahmud@iut-dhaka.edu

## **Abstract**

The world energy demand is growing steadily as is the emission of greenhouse gases. The efforts to enhance energy consumption can escalate greenhouse pollution yet the technologies used to implement zero-emission process have been inefficient. It has long been considered that the solution for both might be one and the same. The scope of this paper is to discuss an integrated power cycle that employs two power sources, namely solar power and s-CO<sub>2</sub> oxy-combustion cycle. This integrated power conversion system provides zero CO<sub>2</sub> emissions, using renewable energy in the form of concentrated solar power at one end and oxy-combustion of natural gas with carbon capture technology at the other end. The power cycle is different from conventional power cycles in the respect that it uses both renewable and non-renewable energy sources to lessen the latter's consumption. Consequently, this enables the integrated system to avoid CO<sub>2</sub> emissions into the environment while responding to energy depletions at the same time. The analysis will include the efficiency of the integrated system and the resulting reduction in fuel consumption based on their thermodynamic analysis. The results will be analyzed to determine whether the proposed power cycle integrating solar power is compatible from the thermodynamic point of view.

## **Keywords**

s-CO<sub>2</sub> oxy-combustion cycle, Concentrated Solar Power (CSP), Zero emissions, Direct Normal Irradiance (DNI) and Carbon capture.

## **1. Introduction**

Owing to the upsurge in energy consumption across all sectors, people are more eagerly searching for the solution which can reduce energy consumption (Łaciak, Szurlej and Włodek, 2020). Fossil fuel combustion is the main anthropogenic reason for CO<sub>2</sub> emissions, used in power plant and industrial processes. Approximately 80% of CO<sub>2</sub> emissions are attributed to the combustion of fossil fuels. In addition, the CO<sub>2</sub> concentration is increased by 48% since the industrial revolution began. Fossil fuel, coal, natural gas are the responsible characters to increase the concentration (NASA, 2019). Worldwide, non-renewable sources meet 85% of energy demand. According to Forbes, global energy consumption for 2019 is shown in Figure 1. As energy consumption increases 1% each year, a current statement reveals the facts of fossil fuels as per the investigation based on 2015 records, which indicates that oil may have a lifespan for nearly 51 years whereas coal up to 114 years and natural gas up to 53 years (MET GRUOP., 2018). Recently, a wave is initiated to reduce CO<sub>2</sub> emissions from power generation (Rogelj *et al.*, 2020).

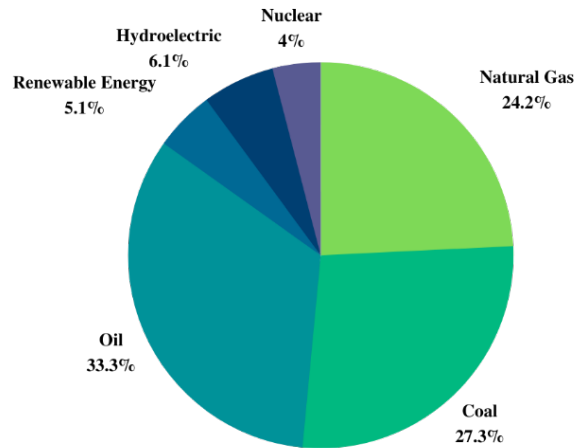


Figure 1. energy consumption statistics(Information 2021)

To achieve a major reduction of CO<sub>2</sub> emissions from power cycle, more focus is on employing clean energy. The main objective is to employ technologies to increase power generation while reducing CO<sub>2</sub> emission. Many countries are already started altering their power generation from non-renewable to renewable which is based on mainly solar, wind, hydro-electric and biomass system, but still there are some challenges related with reliability and cost when it comes to the large-scale deployment (Allam *et al.* 2013). One problem associated with solar energy is the intermittency of solar irradiance, which cause a disruption in power generation from solar. Also, other than intermittency problem, solar photovoltaic (PV) and CSP need thermal storage to solve this stability issue. CSP takes almost 10% of total cost to utilize thermal energy storage (Sector 2012). In this way, the possible solution would be combining renewable and non-renewable energy which left no way other than capturing supercritical CO<sub>2</sub> for fossil fuel power plants which can be called CCS (carbon capture and storage) (Finkenrath 2011)

Oxy-fuel combustion employs sCO<sub>2</sub> as the working fluid and oxygen in the combustion chamber rather than air to eliminate the formation of deadly NO<sub>x</sub> as well as increase CO<sub>2</sub> concentration for storage environment. This s-CO<sub>2</sub> cycle is commonly referred to as the Allam Cycle by NET Power, which will be discussed further below. Interest in s-CO<sub>2</sub> has been increased in recent years because of its unique features like high thermal efficiency and making less pollution to the environment. According to the proposal of Feher (Dostal and Driscoll *et al.* 2004) and Angelino (Configurations 2016) the s-CO<sub>2</sub> cycle is utilized in numerous functionalities such as solar power (Wang and He 2017; Tesio, Guelpa and Verda, 2020) nuclear reactors (Hu *et al.* 2015), waste heat recovery (Liu, Yang and Cui, 2020), oxy-combustion cycles etc. A lot of research has been done already regarding analysis of the underlying thermodynamics principle of s-CO<sub>2</sub>. However, none has followed the path to solve the energy and exergy of the cycles while integrating with concentrated solar power.

### 1.1 Objectives

In this study, we focus to integrate the conventional s-CO<sub>2</sub> cycle with concentrated solar power in order to reduce the fuel consumption of fossil fuel by using CSP technology. Using solar power and recuperator, the turbine inlet temperature will be higher as well as intermittency problem would be solved which eventually increase the thermal efficiency. By utilizing solar power, percentage of reduction of fuel consumption on a monthly basis is also shown in the last part of the paper.

## 2. Literature Review

The patented NET Power cycle utilizes carbon dioxide (CO<sub>2</sub>) as the working fluid and executes a single turbine operating at an inlet pressure of 200 bar to 400 bar. The cycle incorporates an oxy-fuel combustor operating at high pressure to combust the fossil fuel in an oxygen flow only. (Allam *et al.* 2013). This system does not require any additional machinery, procedures, or expenditures while achieving very high operational efficiencies. The supercritical Brayton cycle with CO<sub>2</sub> enables the use of exhaust waste energy (S-CO<sub>2</sub>). By examining various S-CO<sub>2</sub>

publications, it was discovered that, under certain circumstances and for certain applications, it is very likely that this technology will perform better than organic Rankine cycles. One of the primary contributors to the promising prospects is the reasonably high cycle efficiency at the turbine inlet's moderate working medium temperatures (450–600°C) (Rogalev et al. 2021).

Another direct-fired, coal-based, solar-hybrid sCO<sub>2</sub> power cycle is proposed. As asserted, the raw coal is at first dried by N<sub>2</sub>, which has been combusted by the compressed air in the nitrogen heater (NH) of ASU. The solar gasifier's syngas warms the regenerated sCO<sub>2</sub> stream while also drying out the required water for gasification. The proposed solar hybrid system in the paper uses less auxiliary power than the conventional system because it doesn't require oxygen to gasify coal (Xu et al. 2019).

Numerous studies on the operating circumstances of the CSP plant have been conducted in a variety of geographic locations with varying climatic conditions. Teleszewski et al. conducted an analysis of the suitability of parabolic trough CSP plants. The results showed that geographic location had a substantial effect on the CSP operating performance. A full analysis of the Moroccan Noor-I parabolic trough CSP facility was performed by Aqachmar et al. In three different locations in Egypt, Mohamed et al. investigated the effects of plant site location on the performance of CSP plants using molten salt TES. According to Fahad et al. thermodynamic comparison of five S-CO<sub>2</sub> cycle, with a value of 52%, the recompression Brayton cycle was able to reach the best thermal efficiency. Four distinct supercritical CO<sub>2</sub> Brayton cycle layouts were subjected to energy and exergy evaluations by Padilla et al. (simple, recompression, partial cooling with recompression, and recompression with main compression intercooling), the results showed that the recompression with the main compression intercooling Brayton cycle performed the best. The open literature on solar energy technologies contains a sizable number of reviews. For instance, While Parida, Iniyar, and Shubbak investigated solar PV technologies, Fernandez et al. and Islam et al. examined mainstream CSP. Reviews on the individual CSP aided technologies are also available, including reviews on methane reforming by Ozalp et al., solar gasification by Puig-Arnavat et al., and the solar thermo-chemical cycle by Agra-fiotis et al. (Rogelj et al. 2020).

### **3. Methodology**

#### **3.1 Configuration of the CSP-integrated S-CO<sub>2</sub> Oxy-Combustion Cycle**

Whereas conventional power plant cycles are using water or steam to generate power, the s-CO<sub>2</sub> oxy-combustion cycle employs CO<sub>2</sub> as the working fluid with CC technology. The supercritical CO<sub>2</sub> oxy-combustion system has recently been developed to boost the performance of power generation. The s-CO<sub>2</sub> power cycle has prompted a lot of interest due to its advantages of reduced compression work. Here, in this study the paper intends to use both CSP cycle and s-CO<sub>2</sub> oxy-combustion direct cycle to analyze the performance of the combined cycle. The integrated cycle will overcome the inherent challenges of solar intermittency and eliminate the requirement for a thermal storage system. To improve the overall performance, the proposed system incorporates solar thermal heat using CSP reflectors.

#### **3.2 Cycle Description**

The cycle consists of a compressor, turbine, recuperator, solar heat exchanger, combustion chamber and cooler. The following processes take place:

- **Process 1-2:** Compression Stage where cooled CO<sub>2</sub> is pressurized with a compressor isentropically.
- **Process 2-3 and 6-7:** Recuperator stage where cold side CO<sub>2</sub> is preheated at process 2-3 and hot side CO<sub>2</sub> releases heat at process 5-6. The pressure remains constant throughout the processes.
- **Process 3-4:** Constant pressure heat addition through solar heat exchanger, which CSP will provide. Heat loss is negligible. CSP heat helps the working fluid consume lesser amount of fuel.
- **Process 4-5:** Constant pressure heat addition. Main heat exchanger, where combustion takes place.
- **Process 5-6:** Isentropic expansion through turbine. High pressure and high temperature CO<sub>2</sub> is directed to the turbine, pressure and temperature drop, part of the energy is used to produce work.
- **Process 7-1:** Constant pressure heat rejection to the cooler.

#### **3.3 Thermodynamic Modeling with Assumptions**

To analyze the efficiency of the s-CO<sub>2</sub> oxy-combustion cycle in combined with CSP cycle, it is necessary to construct a thermodynamic model of the integrated cycle. A few assumptions should be addressed before developing the mathematical model to remove the complexity of the model.

**Assumptions:**

1. As for primary estimation, all devices are operated at steady state condition.
2. The pressure drop in the pipe and heat exchanger are negligible.
3. Kinetic and potential energies are neglected throughout the cycle.
4. The inlet temperature of the turbine and exit temperature of the cooler are constant.
5. In a water separator, all moisture is eliminated apart from the volume of water beneath saturated water vapor pressure.
6. It is considered that the CO<sub>2</sub> storage area is located downstream of the compressor.
7. Turbinemustsatisfythefollowingequations 1 &2.

$$P_{TurbineOutlet} * PR_{Turbine} - P_{TurbineInlet} = 0 \tag{1}$$

$$T_{TurbineOutlet} = T \{ (1 - Eff_{Turbine}) * h (T_{TurbineInlet}, P_{TurbineInlet}) + Eff_{Turbine} * h [P_{TurbineOutlet}, S (T_{TurbineInlet}, P_{TurbineInlet})], P_{TurbineOutlet} \} \tag{2}$$

8. Compressor must satisfy the following equations 3 & 4.

$$P_{Comp Outlet} - PR_{Comp} * P_{CompInlet} = 0 \tag{3}$$

$$T_{CompOutlet} = T \{ h (T_{CompInlet}, P_{CompInlet}) + 1/Eff_{MC} \{ h [P_{CompOutlet}, S (T_{CompInlet}, P_{CompInlet})] - h (T_{CompInlet}, P_{CompInlet}) \}, P_{CompOutlet} \} = 0 \tag{4}$$

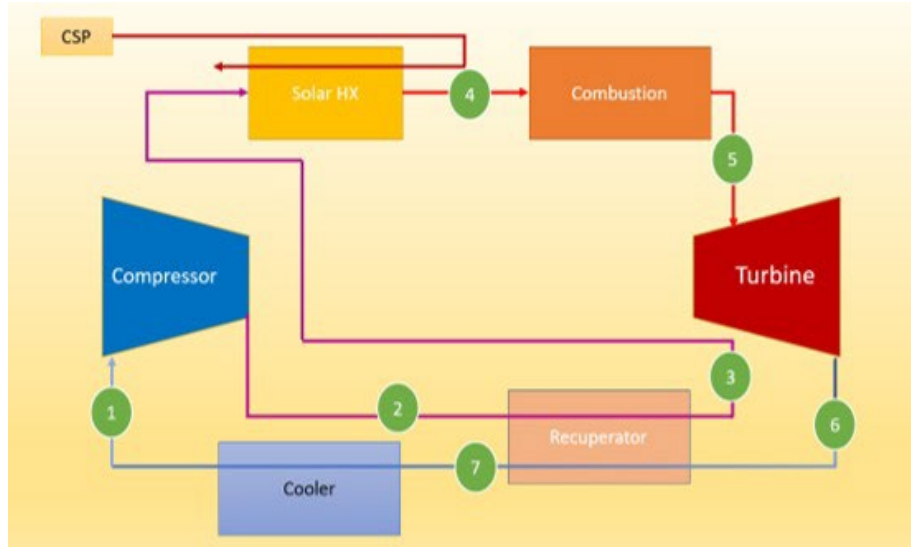
The thermophysical properties of CO<sub>2</sub> may be computed using two parameters and the properties of s-CO<sub>2</sub> were calculated through the CoolProp database. The mathematical equations have been solved through MATLAB integrated with python. The simple recuperated s-CO<sub>2</sub> power cycle input parameters was employed in the estimation shown in Table 1.

Table 1. Input parameters used for thermodynamic analysis (Son *et al.* 2019)

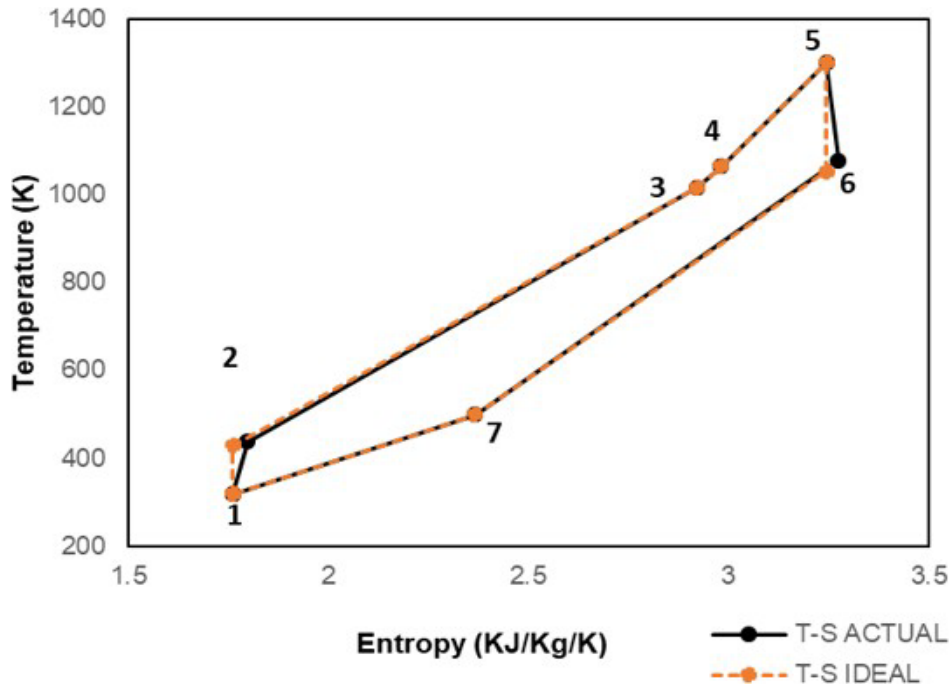
| Parameters   | Value                 | Parameters                          | Value                 |
|--|-----------------------|-------------------------------------|-----------------------|
| Absorptance, $\gamma$                              | 0.95                  | System Maximum pressure             | 30 MPa                |
| Thermal Emittance, $s$                             | 0.85                  | System Maximum Temperature          | Optimized (1300 ° C)  |
| Radiation view factor, $F_{view}$                  | 1                     | System Minimum Temperature          | 45 ° C                |
| Convective heat transfer coefficient, $h_{conv}$   | 10 W/m <sup>2</sup> K | Compressor Isentropic Efficiency    | 80%                   |
| Convective heat loss factor, $f_{conv}$            | 1                     | Turbine Isentropic Efficiency       | 90%                   |
| Annular heliostat field efficiency, $\eta_{field}$ | 0.6                   | Recuperator Effectiveness           | 90%                   |
| Concentration ratio, $C$                           | 900                   | Turbine Pressure Ratio              | Optimized (4)         |
| Solar receiver temperature approach, $\Delta T_R$  | 150 K                 | Direct Normal Irradiance, $E_{DNI}$ | 1100 W/m <sup>2</sup> |
| Ambient Temperature, $T_{amb}$                     | 298.15K               | Ratio of solar heat to combustion   | 20%                   |

**3.4 Design Model**

The model of the CSP integrated simple recuperative S-CO<sub>2</sub> oxy-combustion cycles at design conditions is formulated. Previous research has shown that increasing turbine inlet temperature and pressure, while decreasing compressor inlet temperature, improves the thermal efficiency. Some configurations are tweaked to obtain the best thermal efficiency. Our CSP integrated thermodynamic cycle & T-S diagram are depicted in following Figure 2.



(a)



(b)

Figure 2. (a) Thermodynamic Cycle and (b) T-S Diagram of Integrated System

## 4. Data Reduction

### 4.1 Energy Balance Equation

The thermodynamic model for the simple recuperative S-CO<sub>2</sub> cycle is presented elaborately in this study. These following equations are related to the symbols and states represented in Figure 2. As previously stated, the compression stage is assumed to have 80% isentropic efficiency; using pressure & temperature at the compressor's inlet, and pressure at the outlet, the enthalpy of s-CO<sub>2</sub> at stage 2 can be calculated by equation 5.

$$W_{1-2} = m_{CO_2} \cdot (h_2 - h_1) \quad (5)$$

Where,

$W_{1-2}$  = Required compressor power (W)

$h_2$  = Specific enthalpy of CO<sub>2</sub> at the compressor outlet (KJ/kg)

$h_1$  = Specific enthalpy of CO<sub>2</sub> at the compressor inlet (KJ/kg)  $m_{CO_2}$  = mass stream of CO<sub>2</sub> (kg/s)

The next stage is the recuperator stage. The thermal efficiency increases due to regeneration. Consequently, less heat is needed to generate the same amount of work (YUNUS A. et al., 2018). Effectiveness of the recuperator,

$$\epsilon_R = (h_3 - h_2)/(h_6 - h_2) \quad (6)$$

Where,

$h_3$  = Specific enthalpy of CO<sub>2</sub> at the recuperator outlet (KJ/kg)  $h_2$  = Specific enthalpy of CO<sub>2</sub> at the recuperator inlet (KJ/kg)

$h_6$  = Specific enthalpy of CO<sub>2</sub> at the recuperator inlet (KJ/kg)

After circulating from the recuperator, S-CO<sub>2</sub> will arrive at the power cycle's new integration itself. Supercritical CO<sub>2</sub>, which is used in the advanced power cycles under consideration for CSP, can achieve higher efficiency at lower costs than steam-based cycles. With its solar heat exchanger, the CSP system helps keep things moving forward by improving inlet temperature. The thermodynamic properties of S-CO<sub>2</sub> at this stage can be calculated using the first law of thermodynamics.

Energy Released by the solar heat exchanger = Energy utilized to heat the working fluid passing through the solar heat exchanger. Taking the additional heat from the solar heat exchanger, the working fluid, S-CO<sub>2</sub> attains more heat by combustion of Methane and Oxygen in the combustion chamber. To generate mechanical energy, CO<sub>2</sub> is passed through the turbine at the next stage of this process. To proceed, the analysis implies a pressure where CO<sub>2</sub> will be expanded. Considering the compressor's inlet pressure (turbine outlet pressure will be same as compressor inlet pressure if there's no pressure drop) as well as the turbine's inlet pressure and temperature, it is possible to compute the actual temperature of CO<sub>2</sub> after expansion.

$$T_6 = T_5 - \eta_T \cdot (T_5 - T_{6S}) \quad (7)$$

Where,

$T_6$  = Actual temperature of CO<sub>2</sub> after expansion (K)  $T_5$  = Temperature of CO<sub>2</sub> at the turbine's inlet (K)

$T_{6S}$  = Ideal temperature of CO<sub>2</sub> after expansion (K)  $\eta_T$  = Isentropic efficiency of the turbine

The S-CO<sub>2</sub> specific enthalpy at stage 6 is calculated using the temperature and pressure of CO<sub>2</sub> at the turbine exit. As a result, the power output can be computed using the equation.

$$W_{5-6} = m_{CO_2} \cdot (h_6 - h_5) \quad (8)$$

Where,

$W_{5-6}$  = Required compressor power (W)  $h_6$  = Specific enthalpy of CO<sub>2</sub> at the turbine outlet (KJ/kg)

$m_{CO_2}$  = Mass of CO<sub>2</sub> (kg/s)  $h_5$  = Specific enthalpy of CO<sub>2</sub> at the turbine inlet (KJ/kg)

By the following equation, the total power of the system is expected to be turbine shaft power omitting compressor power.

$$W_{net} = W_{5-6} - W_{1-2} \quad (9)$$

Where,

$W_{net}$  = The net power of the system (KW),  $W_{1-2}$  = Required compressor power (KW)

$W_{5-6}$  = The power on the turbine shaft (KW)

The cooler stage is the final stage of the model calculation. Assuming the zero pressure drop of the cooler, therefore both the compressor and the cooler maintain the same inlet pressure. Depending on the S-CO<sub>2</sub> pressure and enthalpy in step 7, the method calculates the cooler's inlet temperature using the CoolProp database. The equation 7 is utilized to evaluate the CO<sub>2</sub> enthalpy value at stage 7.

$$h_7 = h_6 - (h_3 - h_2)/\eta_R \quad (10)$$

Where,

$h_7$  = Specific enthalpy of CO<sub>2</sub> at the recuperator hot side outlet (KJ/kg)  $\eta_R$  = Recuperator Effectiveness

$h_6$  = Specific enthalpy of CO<sub>2</sub> at the recuperator hot side inlet (KJ/kg)       $h_3$  = Specific enthalpy of CO<sub>2</sub> at the recuperator cold side outlet (KJ/kg)  
 $h_2$  = Specific enthalpy of CO<sub>2</sub> at the recuperator cold side inlet (KJ/kg)

The thermodynamic performance of the S-CO<sub>2</sub> cycle might be assessed using energy and exergy analyses. Thermal efficiency of the cycle is evaluated from the following equation and it appears to be around 55.64%.

$$\eta_{th,eff} = \frac{W_{net}}{Q_{in}} \quad (11)$$

Where,

$\eta_{th,eff}$  = Thermal efficiency

$W_{net}$  = The net power of the integrated cycle

$Q_{in}$  = Total heat added in the power cycle

## 5. Results and Discussion

### 5.1 Model Validation

The calculations of this simple recuperative CSP integrated oxy-combustion cycle under design conditions is evaluated by the results of paper (Son et al., 2019). The cycle efficiency with CSP integrated has been examined and the results are presented in the Figure 3. The findings of this investigation are consistent with those of paper (Son et al. 2019).

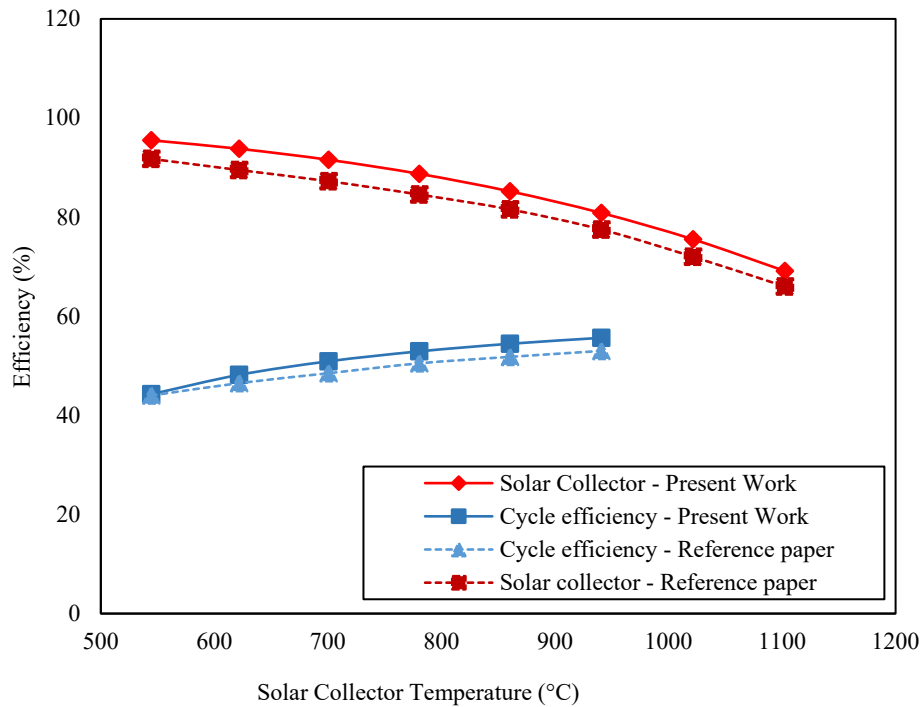


Figure 3. The efficiency of the integrated power cycle

Table 2. Validation results of the efficiency of and CSP integrated power cycle

| Solar Collector Temperature (°C) | Cycle Efficiency, (%) |               | Error (Cycle Efficiency, %) | Solar Collector, (%) |               | Error (Solar Collector), (%) |
|----------------------------------|-----------------------|---------------|-----------------------------|----------------------|---------------|------------------------------|
|                                  | Ref. Paper            | Present Study |                             | Ref. Paper           | Present Study |                              |
| 544.42                           | 44                    | 44.27         | 0.62                        | 91.75                | 95.5          | 4.08                         |
| 621.78                           | 46.5                  | 48.17         | 3.59                        | 89.5                 | 93.79         | 4.79                         |

|         |      |       |      |       |       |      |
|---------|------|-------|------|-------|-------|------|
| 700.51  | 48.5 | 50.9  | 4.95 | 87.25 | 91.57 | 4.95 |
| 780.49  | 50.5 | 52.91 | 4.77 | 84.55 | 88.72 | 4.94 |
| 860.28  | 51.8 | 54.44 | 5.1  | 81.55 | 85.2  | 4.47 |
| 940.75  | 53   | 55.64 | 4.98 | 77.5  | 80.83 | 4.3  |
| 1021.52 | -    | -     | -    | 72    | 75.52 | 4.89 |
| 1102.4  | -    | -     | -    | 66    | 69.13 | 4.75 |

Here the Figure 3 illustrates the efficiency changes in the integrated power system according to the solar collector temperature. Equation 1-4 were used to calculate these results. Calculation parameters can be found in Table 2.  $E_{DNI}$  values are considered high in Table 2 in order to make the idea easier to grasp using an ideal example.

### 5.2 Solar to Work Efficiency

The dissipation from radioactivity is one of the most important thermodynamic considerations of CSP. Due to heat loss from radiation, the central CSP receiver is only capable of transmitting a portion of the available solar energy to the cycle. From this perspective, solar-to-work efficiency ( $\eta_{th}$ ) is a function of solar radiation power and convective heat losses. through radiation and condensation in the equation. (Campus, Campus and Data, 2010).

$$\eta_{th} = 1 - \frac{\varepsilon \sigma F_{view} T_R^4 + f_{conv} h (T_R - T_{amb})}{\eta_{field} E_{DNI} C} \quad (12)$$

To attain high efficiency, high turbine inlet temperature is required. Nevertheless, The amount of energy loss as a result of radiation increases as the solar receiver's temperature rises. So, CSP is not capable of generating significantly higher temperatures at the turbine inlet. The proposed configuration incorporates the oxy-combustion cycle with solar heat obtained by the CSP reflectors to boost efficiency. Using a solar heat exchanger, the CSP system raises the temperature of the combustor's input, contributing to the s-CO<sub>2</sub> cycle. In high temperatures, the combustor can raise the turbine inlet temperature higher while consuming much less fuel. As a result, the system's overall cost can be reduced while maintaining its simplicity and satisfying emission standards under improved cycle performance.

### 5.3 Efficient Power Conversion System

The integration of CSP with sCO<sub>2</sub> oxy-fuel combustion serves two purposes; it solves the intermittency issue of the CSP and it allows the power conversion system to operate at the on-design point condition. Due to the fluctuation of solar irradiance, CSPs must frequently operate at a part load. So, the power it provides at Off-design point conditions is less efficient than the power output at full capacity. When using two power conversion systems to fulfill the everyday grid demand both processes are made to work at a part load. Despite the fact that the required power demand may be supplied, the efficiency of each power conversion system falls since to boost efficiency, the thermodynamic system should initiate with a high temperature at the turbine inlet. Integrating CSP with sCO<sub>2</sub> oxy-fuel combustion will help to solve the inefficiency problem because the solar power has the capability to raise the turbine's inlet temperature.

To assess the feasibility and profitability of the proposed system, some preliminary calculations were performed to estimate the reduction of fuel consumption in specific regions with operating CSP plants. The analysis was made using data for the Direct Normal Irradiance (DNI) values across regions with high solar irradiance (Campus, Campus and Data, 2010). To assess the advantages of the integrated thermal power cycle, further calculations were performed where it was assumed that the layout of both the integrated and separated CSP and oxy-combustion system is identical. This assumption is made so that the advantages could be presented in relative terms whereas excluding items that may hinder the cycle performance (Scaccabarozzi, Gatti and Martelli, 2017). The efficiency of the off-design performance was estimated using a second order interpolation shown in the equation 13.

$$\varepsilon_{off} = \varepsilon_{design} (-0.0056L^2 + 1.05L + 5) \quad (13)$$

L represents the ratio between the design and off-design loads. Figure 4 shows the estimation of the off-design point efficiency relative to the thermal load provided. The x-value (thermal load) corresponds to L and the Normalized



System Efficiency is the off-design efficiency relative to the thermal efficiency of thermodynamic model. The graph follows a trend, which indicates that increasing the thermal load given to the power conversion system increases its efficiency and the calculated data is compared with the paper's reference amount of fuel consumption reduction.

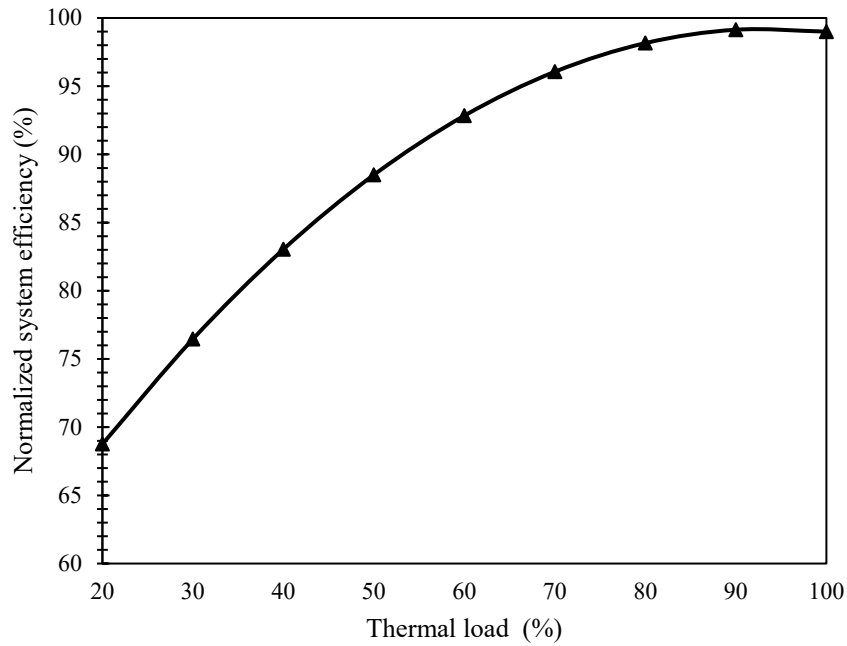


Figure 4. Part-load performance of s-CO<sub>2</sub> power conversion system

The data in figure is then used in combination with off-design performance system in equation 13 and DNI data from various regions. The electricity demand is assumed to be constant (base load) and the value is based on the maximum DNI value obtained on a day in a specific region. Another assumption made during this calculation was that the solar heat output obtained in a day depends on the DNI value, and the rest of the output power is produced from combustion. Based on this assumption it can be suggested that the proposed integrated system helps to cut down on the amount of fuel required to supply the demand for electricity.

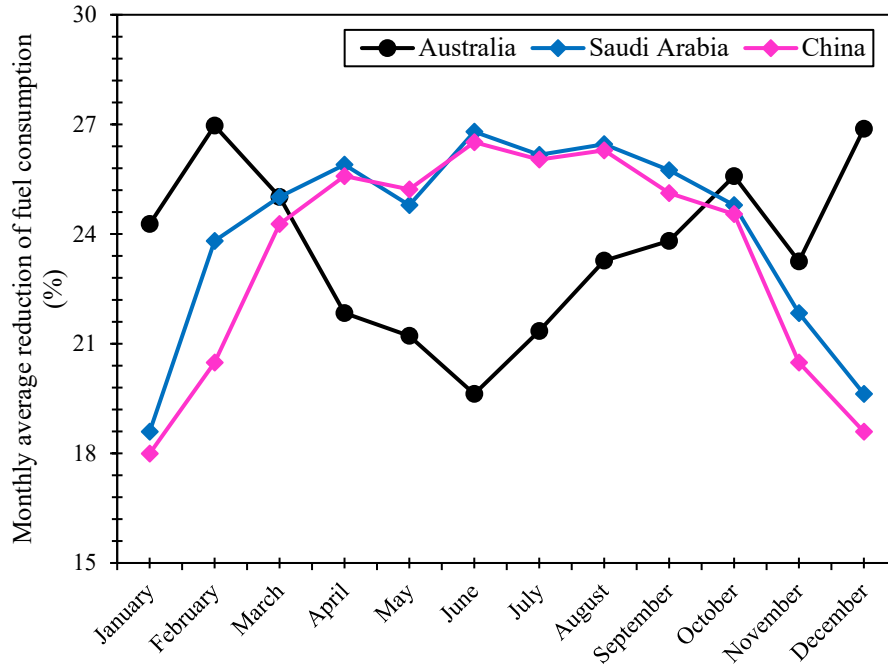


Figure 5. Reduced monthly average fuel consumption in different areas

Figure 5 depicts the scenario of the reduced fuel consumption after integration of CSP cycle with s-CO<sub>2</sub> oxy combustion cycle in a month. The results reveal that the more sunlight there is, the larger the effects of the integrated system. The estimated amount of fuel utilized in the reference scenario is 18–28% less.

Figure 10 depicts the histogram profile of fuel consumption reduction. According to the findings, the integrated system possesses more cost-effective days near the equator compared to the separated one.

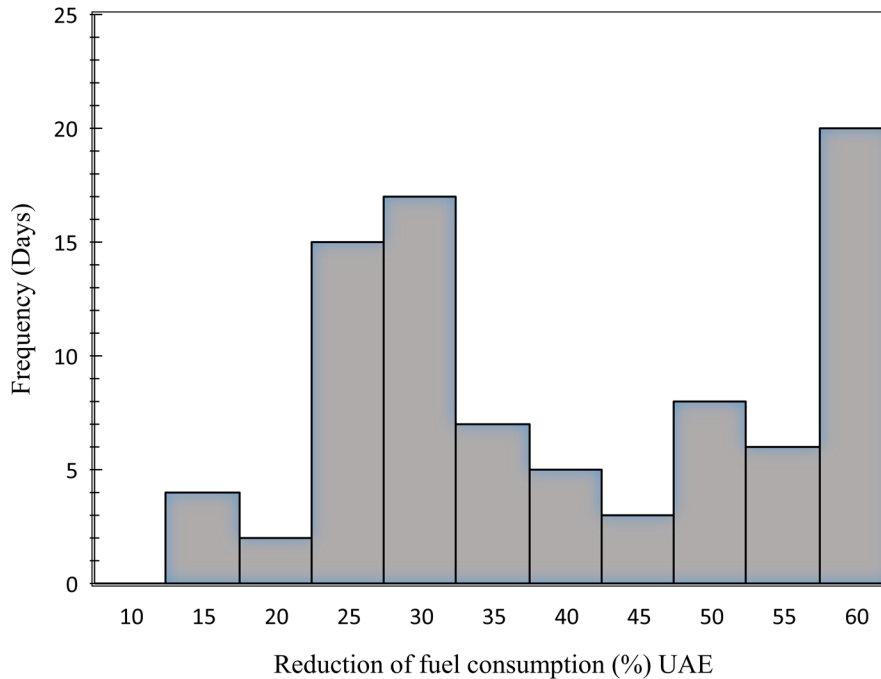


Figure 6. Histogram profile of the reduction of fuel consumption

## 5.4 Future Recommendations

By performing the thermodynamic analysis of the CSP integrated cycle, it was ascertained that this integrated cycle has higher thermal efficiency along with the reduction of required fuel substantially. Based on the foregoing assessment, several recommendations for the integrated cycle can be accomplished. The optimized parameters for achieving maximum thermal efficiency are one of the most significant aspects for cost effectiveness of power plants. In addition, conducting an exergoeconomic analysis of the cycle can disclose the relative cost significance of each element and the possibilities to improve the overall cost efficiency. To obtain an overview of the distinctive concept of the integrated power plant, the proposed cycle should be reviewed in other CSP locations not mentioned in this paper. Meanwhile, Allam cycle, one of the s-CO<sub>2</sub> oxy-combustion cycle offers several benefits, including the simplicity of CO<sub>2</sub> storage and environment friendly that will eventually play a vital role in reducing global temperature. The in-depth explanation of this is beyond the focus of this specific study, but further research is required because it may reduce the overall cost.

## 6. Conclusion

The work has demonstrated an approach to integrate CSP system with an s-CO<sub>2</sub> oxy-combustion system. This innovation's compelling feature is that it emits no carbon while surpassing most power plants and utilizing solar energy more effectively than traditional solar power plants. As a result, it reduces the fuel consumption significantly; this feature makes the system feasible to be used in many regions of the world where the potential for solar heat is greater. This report includes some preliminary calculations and their graphical representations to support this proposal. The data obtained from these calculations draws up a comparison between the efficiencies of a solar plant at the on-design condition and off-design condition. The calculations show that the integration not only solves the intermittency of solar heat but it also enables the system to achieve greater efficiency owing to high turbine inlet temperature. In addition, the efficiency is reduced further as the solar plant does not need to operate at part-load to conserve heat and can instead obtain heat from combustion. All of these advantages cumulate to reduce the fuel consumption significantly in comparison to a separated system.

## Reference

- Allam, R.J. and Palmer, R., High efficiency and low cost of electricity generation from fossil fuels while eliminating atmospheric emissions, including carbon dioxide, *Energy Procedia*. Elsevier, vol. 37, pp. 1135–1149, 2013.
- Campus, M. and Data, J., Estimation of hourly averaged solar irradiation : evaluation of models, vol. 1, pp. 9–25, 2010.
- Dostal, V., Driscoll, M. J. and Hejzlar, P., Advanced Nuclear Power Technology Program A Supercritical Carbon Dioxide Cycle for Next Generation Nuclear Reactors, 2006.
- Finkenrath, M., Cost and Performance of Carbon Dioxide Capture from Power Generation, 2011.
- Hu, L., Investigation on the performance of the supercritical Brayton cycle with CO<sub>2</sub>-based binary mixture as working fluid for an energy transportation system of a nuclear reactor, pp. 1–13, 2015.
- Today in Energy, Available at: <https://www.eia.gov/todayinenergy/detail.php?id=49876>, October 7, 2021.
- Łaciak, M., Szurlej, A. and Włodek, T., A Case Study of the Supercritical CO<sub>2</sub>-Brayton Cycle at a Natural Gas Compression Station, *Energies*, 2020.
- Liu, L., Yang, Q. and Cui, G., Supercritical Carbon Dioxide(s-CO<sub>2</sub>) Power Cycle for Waste Heat Recovery: A Review from Thermodynamic Perspective', *Processes*, pp. 1–18, 2020.
- MET GROUP, *WHEN WILL FOSSIL FUELS RUN OUT?* Available at: <https://group.met.com/fyouture/when-will-fossil-fuels-run-out/68>, 2018.
- The Causes of Climate Change, Available at: <https://climate.nasa.gov/causes/>, 2020.
- Rogalev, A., Cycles with CO<sub>2</sub> Recirculation, *Energies*, pp. 1–18, 2021.
- Rogelj, J., Paris Agreement climate proposals need a boost to keep warming well below 2°C, *Nature*, pp. 631-639, 2016.
- Scaccabarozzi, R., Gatti, M. and Martelli, E., Thermodynamic Optimization and Part-load Analysis of the NET Power Cycle, *Energy Procedia*, pp. 551–560, 2017.
- Son, S., Reduction of CO<sub>2</sub> emission for solar power backup by direct integration of oxy-combustion supercritical CO<sub>2</sub> power cycle with concentrated solar power, *Energy Conversion and Management*. Elsevier, 2019.
- Tesio, U., Guelpa, E. and Verda, V., Energy Conversion and Management : X Integration of thermochemical energy storage in concentrated solar power . Part 1 : Energy and economic analysis / optimization, *Energy Conversion and Management: X*. Elsevier, 2020.
- Wang, K. and He, Y., Thermodynamic analysis and optimization of a molten salt solar power tower integrated with

a recompression supercritical CO<sub>2</sub> Brayton cycle based on integrated modeling, *Energy Conversion and Management*. Elsevier Ltd, vol.135, pp. 336–350,2017.

Xu, C., A thermodynamic analysis of a solar hybrid coal-based direct-fired supercritical carbon dioxide power cycle, *Energy Conversion and Management*. Elsevier, vol. 196, pp. 77–91, 2019.

Yunus, A., *Thermodynamics And Engineering Approach*, 8<sup>th</sup> Edition, 2018.

## **Biographies**

**Foyez Ahmad** has recently graduated from Islamic University of Technology (IUT), Gazipur, Bangladesh with B.Sc. degree in Mechanical Engineering. His research interest includes thermal power generation, heat transfer and renewable energy sectors. He is a member of the Institution of Mechanical Engineers (IMEchE) and the American Society of Mechanical Engineers (ASME).

**FardinMahatab** is a graduate student from the department of Mechanical and Production Engineering (MPE) at Islamic University of Technology (IUT), Gazipur, Bangladesh. His research interests include machine learning, autonomous systems, spacecraft propulsion and fluid mechanics.

**Sajjad Mahmud** has recently obtained his B.Sc. in Mechanical Engineering from Islamic University of Technology. He is now working as an Executive Engineer at Navana Limited-Toyota Bangladesh. He is also a member of the Institution of Mechanical Engineers (IMEchE) and the American Society of Mechanical Engineers (ASME). His research interests include computational fluid dynamics, automobile engineering, power plant engineering, and fluid mechanics.